Materials Research Proceedings 35 (2023) 127-134 https://doi.org/10.21741/9781644902714-16

LPBF process of Zn-modified NiTi alloy with enhanced antibacterial response

Carlo Alberto Biffi[1,a*], Jacopo Fiocchi[1,b], Francesca Sisto[2,c], Chiara Bregoli[1,d], Ausonio Tuissi[1,e]

[1] National Research Council of Italy - Institute of Condensed Matter Chemistry and Technologies for Energy, Via Previati 1E, 23900 Lecco, Italy

[2] University of Milan, Department of Biomedical, Surgical and Dental Sciences, Milan, Italy

[a]carloalberto.biffi@cnr.it, [b]jacopo.fiocchi@cnr.it, [c]francesca.sisto@unimi.it, [d]chiara.bregoli@icmate.cnr.it, [e]ausonio.tuissi@cnr.it

Keywords: Additive Manufacturing, Laser Processes, Shape Memory Alloy

Abstract. In this work the use of Laser Powder Bed Fusion (LPBF) process enabled the development of customized implants with advanced functional materials for the biomedical sector. In details, Ni rich NiTi Shape Memory Alloy (SMA) powder, mixed with Zn powder, were used for building samples, able to couple the typical superelasticity of the initial material with the antibacterial response, offered by the dopant element. The main parameters of the LPBF process were revised for achieving full dense parts. Further, the functional performances of the novel NiTiZn SMA were analyzed and compared with the ones of the reference material. Finally, the antibacterial response against different bacteria was tested. It was found a promising antibacterial response against Staphylococcus aureus of the NiTiZn SMA, while the addition of Zn into NiTi did not supress the martensitic transformation of the NiTi alloy and allowed to maintain the superelastic recovery.

Introduction

Shape Memory Alloys (SMAs) are smart and functional materials, which are well known for their unique thermo-mechanical properties, namely shape memory effect (SME) and superelasticity (SE) [1]. Among SMAs, the near-equiatomic intermetallic NiTi compound exhibits optimal SME and SE characteristics and it finds extensive application fields, particularly the biomedical one [2]. Ni-rich NiTi alloys offer some suitable properties for developing of implantable elements, including good biocompatibility, adjustable elastic modulus and the ability of supporting early ingrowth of bone [2,3]. However, a dangerous issue that may trigger the failure of metallic implants, including the use of NiTi alloys, regards the occurrence of post-surgery bacterial infections [4]. This makes the development of antibacterial implants highly auspicious in the view of limiting the occurrence of post-surgery infections troubles. The choice of bioactive surface modifications of NiTi implants have been developed, which often exploit the inherent antibacterial properties of some inorganic elements, such as Ag, Cu, Zn and Ga [5]. Among these elements, Ag is the most investigated as coating in the form of nanoparticles on NiTi surfaces [6-8], whereas Zn seems to be highly promising, since it couples excellent osteogenic ability and favourable antibacterial response [9-10].

All these opportunities in the use of advanced and novel materials need to be well connected with the best choice of manufacturing process routes. Nowadays, bone implants can be manufactured through Additive Manufacturing (AM) technology, which lead to high degree of shape complexity and customization, very important for improving the implant performance and to treat better and faster the patience issue. The use of AM for manufacturing NiTi SMAs have been largely investigated in literature. Several works demonstrated the feasibility of Ti rich and Ni

Materials Research Proceedings 35 (2023) 127-134 https://doi.org/10.21741/9781644902714-16

rich NiTi alloys and the investigation regarding the evolution of their functional behaviour with respect to the conventional method of manufacturing. In particular, among AM technologies the most challenging one for processing NiTi powders is Laser Powder Bed Fusion (LPBF), in which a laser beam is adopted for promoting a rapid melting of the powder bed. Probably the most critical aspect to be mentioned for the LPBF process of these smart alloys regards the requirement of precise control of both the chemical composition (i.e. Ni/Ti ratio) and the obtained microstructure: these have a huge impact on the functional behaviour [11]. Therefore, the modification of the composition of 3D built parts for tuning the functional properties is a very challenging topic but just few works have been done in this area.

Under this light, the present work is oriented to investigate the effect of the addition of Zn into Ni rich NiTi SMA powder on the LPBF processability and on the functional and antibacterial response of the built samples.

Experimental

Materials

Two types of powders, obtained from Ni56Ti46 (wt.%) and pure Zn powders (see Figure 1), were used for the LPBF process: (i) Ni rich NiTi powder; and (ii) NiTi mixed with 2% in weight of Zn, from here named as NiTiZn. Such mixture was prepared with a powder mixer working for 2 hours under argon atmosphere; its chemical homogeneity was checked by compositional analysis.

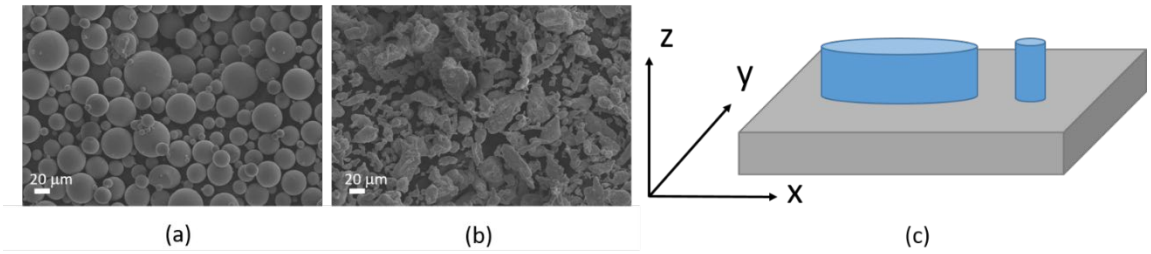

Figure 1: NiTi (a) and Zn (b) powders; schematic depicting the built samples (c).

LPBF process

Samples with NiTi and NiTiZn powders were manufactured by means of a LPBF system (mod. AM400 from Renishaw), equipped with a pulsed wave (PW) laser with a maximum power of 400 W and a reduced build volume (75 mm x 75 mm x 50 mm). The schematic of the PW emission mode is depicted in Figure 2, where the principal energetic and spatial features are reported.

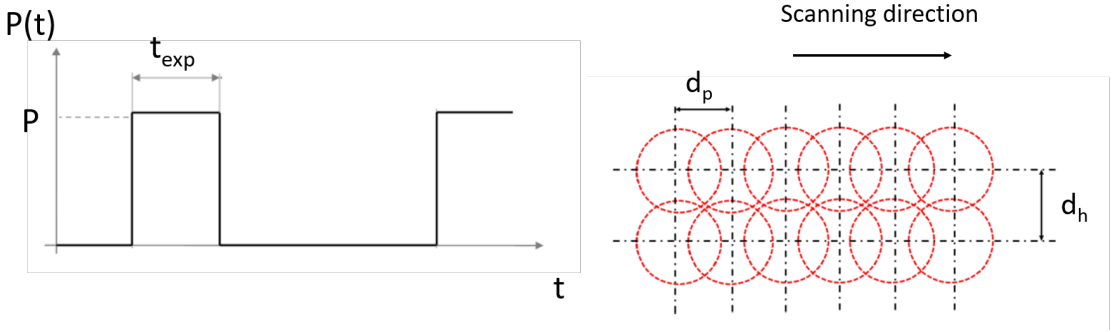

Figure 2: Schematic of the temporal power profile and spatial pulses path (b) in SLM performed with PW emission mode [14].

Materials Research Proceedings 35 (2023) 127-134 https://doi.org/10.21741/9781644902714-16

LPBF process conditions, which are reported in Table 1, were investigated for studying the feasibility of the NiTiZn powder, having the aim of maximizing the relative density. The same process conditions were also investigated for printing NiTi powder, as reference. A full factorial design was adopted at varying both laser power and exposure time, as suggested in Table 1; three replicas for each process condition were carried out for estimating the variability of the LPBF process. Cylindrical samples (3 mm in diameter and 5 mm in height) were realized for density measurements, metallographic analyses and compressive testing. Moreover, disc samples (10 mm in diameter and 3 mm thick) for antibacterial testing were also produced on the NiTi platform, as show in Figure 1c.

Table 1: Variable and fixed process parameters used for printing NiTi and NiTiZn samples.

Parameters		**Values**
Variable parameters	Power	150-160-170 W
	Exposure time	75-100-125 μs
Fixed parameters	Scanning strategy	Meander
	Atmosphere	Argon
	Layer thickness	30 μm
	Hatch distance	50 μm
	Point distance	50 μm
	Laser spot size	65 μm
	Platform temperature	30°C
	Tilting angle	67°
	Oxygen level	< 20 ppm

Density and metallurgical characterization

Part relative density was measured by Archimedes's principle using a Gibertini E50S2 precision digital balance for each cylindrical sample, considering a full density of 6.45 g/cm3.

X-ray micro Computed Tomography (μ-CT) was performed on selected cylindrical samples, having the highest relative density value for each powder batch. A XTH225 –ST system, from Nikon, having an X-ray Gun of 225kV and 16 bits flat panel Varex 4343CT as detector, was adopted to highlight the defects within the entire volume of the sample.

Martensitic transformation temperatures of the two alloys were investigated by differential scanning calorimetry (DSC, TA Instrument Q25) at 10 °C/min heating/cooling scan rate. Compositional analysis was carried out by Scanning Electron Microscopy (SEM, mod. LEO), coupled with energy Dispersive X-ray Spectroscopy (EDS) on the external surface and the polished surface, respectively. Compressive tests were conducted at 25°C by means of an MTS Exceed E45 machine, equipped with extensometer, at strain rate of 0.01 min-1.

Antibacterial characterization

Finally, antibacterial testing was carried out on the built discs, by agar slurry according with the standard protocol [15]. Staphylococcus aureus strain (Gram positive, ATCC 29213) and Pseudomonas aeruginosa (Gram negative, ATCC 19660), were used: these bacteria were selected because they are the main causes of prosthetic infections. Three replicas of the test were performed and studied to ensure the repeatability of the study. The bacteria were cultured on agar media and incubated at 37°C for 24 hours. Then, an inoculum of 0.5 McFarland (about 1.5 x 108 Colony Forming Unit/ml - CFU/ml) was prepared in broth and further diluted to obtain a suspension of about 105 CFU/ml in agar slurry medium [16].

Materials Research Proceedings 35 (2023) 127-134 https://doi.org/10.21741/9781644902714-16

Results

LPBF processability

During the laser scan of the powder bed, the energy provided to the powder bed during the LPBF process, namely also fluence, is described, as follow:

$$F = \frac{P * t_{on}}{d_p * d_h * s}$$

where P is the laser power, ton is the exposure time, dp is the point distance, dh is the hatch spacing, and s is the layer thickness.

The typical trend of the relative density versus the laser fluence can be recognized for both the powders' batches, as shown in Figure 3. In details, the relative density exhibits a rapid increase at low laser fluence values, then it can reach its maximum point, in correspondence of the full densification of the powder; upon another increase of the laser fluence, a decrease of the relative density can be found. In details, for NiTi-Zn powder, as low relative density as 95.5% was achieved from 33 J/mm3; a rapid increase was observed up to 99.6% at 44 J/mm3, then also a rapid decrement of the relative density was appreciated suddenly from 98.3% at 47 J/mm3 down to 95% at 62 J/mm3 (see Figure 3a). For NiTi powder, the relative density increased from 98.3% at 33-35 J/mm3 up to 99.4% at 38 J/mm3, then it decreased slowly down to 99% at 47 J/mm3 and quickly down to 96% at 60 J/mm3 (see Figure 3b). It can be stated that the Zn powder shape was irregular, but it did not influence the sample quality during the LPBF process; in fact, the presence of Zn did not counter the high relative density in the building of NiTiZn parts.

The curves reported in Figure 3 represent the main trend on the measurements, and they can be used as a support for the discussion of the achieved results.

Moreover, the laser fluence for producing full dense NiTi-Zn samples is higher than the one for full densification of NiTi powder; this can be explained because of the higher energy required by the complete melting of NiTi and the vaporization of Zn achieved once the NiTi is melted. In fact, the compositional analysis, carried out with SEM-EDS, revealed that no evident traces of Zn were found in the NiTiZn sample. On the contrary, the external surfaces of the sample showed the presence of Zn, probably just partially melted by the laser beam scan, because of different process parameters adopted for the realization of the sample border.

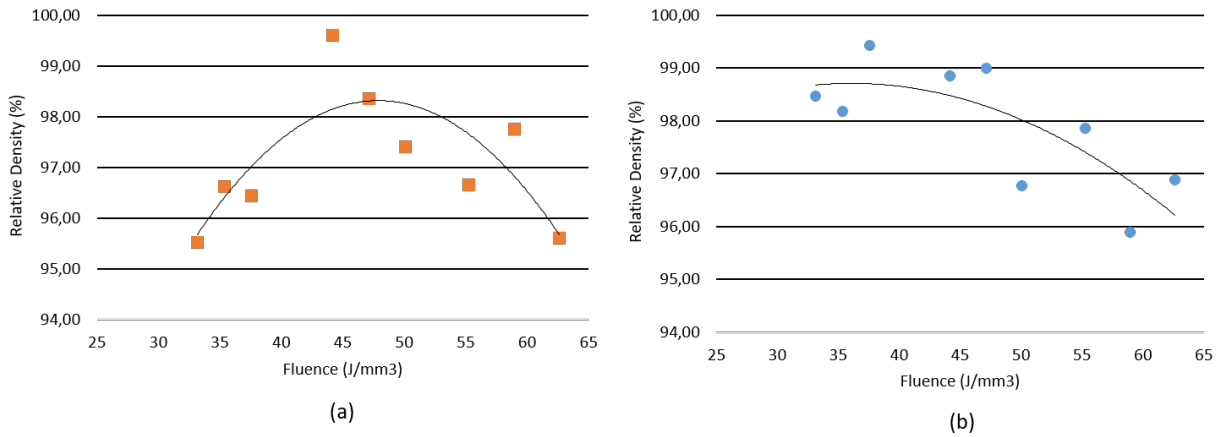

Figure 3: Relative density vs fluence curves for NiTiZn (a) and NiTi (b) powders.

The defects analysis was completed with micro-CT scans of the NiTiZn and NiTi samples. Figure 4 shows the 3D reconstruction of the two samples, in which the detectable defects are highlighted with different colors in function of their size. It can be seen that the NiTiZn sample

Materials Research Proceedings 35 (2023) 127-134 https://doi.org/10.21741/9781644902714-16

exhibited limited amount of defects, just few as large as 300 μm around and characterized by pretty irregular shape: this suggests that the Zn evaporation may induce this type of defects. On the contrary, the NiTi sample showed high number of defects having smaller size and spherical.

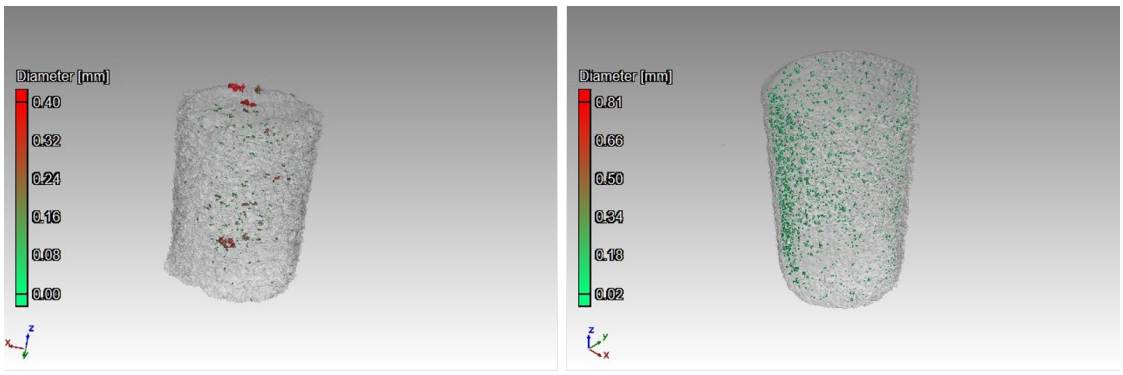

(a) (b)

Figure 4: Micro-CT analysis of the NiTiZn (a) and NiTi (b) samples, built with the selected process conditions.

Both the built samples show the typical phase transformation of the SMAs [17]. Figure 5 depicted the DSC scans where peaks upon heating and cooling were visible. The transformation temperature of the martensitic transformation suggested that both the samples are austenitic at body temperature (i.e. 37°C), indicating that these can show the SE. This result can also indicate that the Ni/Ti ratio was almost not varied by the scanning of the laser beam, avoiding a sensible change of the chemical composition. Additionally to the DSC of the built samples, the one of the initial powder was also analyzed. Here it can be seen that the shape of the peaks of the phase transformation are pretty different: the powder shows a multistage phase transformation, while single stage for the built samples. This could depend on lack of chemical and microstructural uniformity (change of Ni/Ti ratio, residual stresses, change in grain size). Anyways, the transformation temperatures are not slightly change from the power to the built samples, again.

The SE behaviour was tested on the samples, subjected to a low temperature heat treatment, also namely aging, typically carried out on SMAs for promoting the functional performances. In this case, compression testing was carried out at 30°C; each mechanical test was composed by a loading stage up to 6% as maximum strain, followed by an unloading down to 0%. The results are depicted in Figure 6.

It can be clearly seen that the two samples exhibited largely different mechanical behaviour. In particular, the NiTiZn can reach as low stress as 450 MPa at 6% in strain, while the residual strain upon unloading was 1%. This indicates that a strain recovery of 5% was achieved.

Materials Research Proceedings 35 (2023) 127-134 https://doi.org/10.21741/9781644902714-16

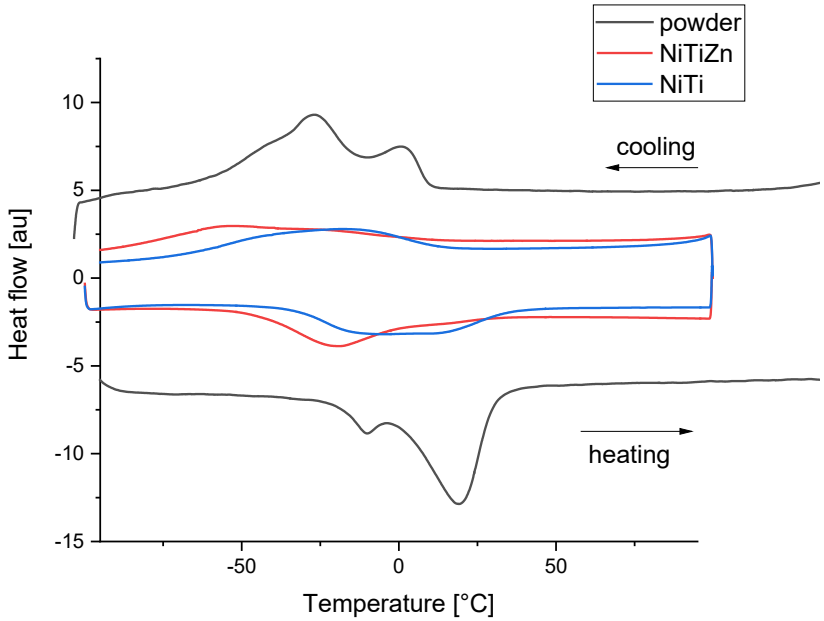

Figure 5: DSC scans of the NiTiZn and NiTi built samples, and the NiTi powder.

On the contrary, the NiTi sample appeared to be less SE, due to a limited strain recovery up to 3%. Moreover, higher maximum stress was achieved up to 1000 MPa for NiTi, while 450 MPa in the case of NiTiZn. These results suggest a higher performance of the NiTiZn sample than the undoped NiTi one.

Finally, the effect of the Zn presence was tested with antibacterial testing. Figure 7 shows the evolution of the bacteria population, Pseudomonas aeruginosa and Staphylococcus aureus, from the beginning of the test (time zero, T0) until 6 hours (T6).

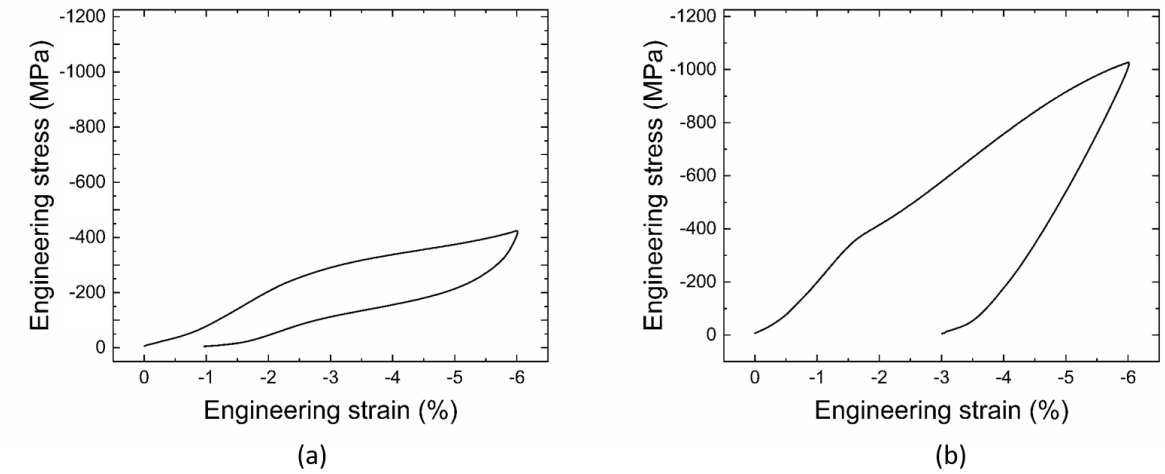

Figure 6: Stress-strain curves of NiTiZn (a) and NiTi (b) built samples, subjected to heat treatment.

It can be seen that the NiTi sample promoted a proliferation of the Pseudomonas aeruginosa bacterium after 6 hours, while the bacterium concentration was constant after the same time (see Figure 7a). On the contrary, the presence of Zn could alter largely the action against the Staphylococcus aureus bacterium after 6 hours, as shown from Figure 7b [17]. Like the previous

case, undoped NiTi sample promoted a large proliferation of the Staphylococcus aureus after 6 hours, while its population was decreased on the surface of the NiTiZn sample. This result suggest an evident antibacterial action of the Zn with respect to Staphylococcus aureus; at the second stage, it is also clear that no bacteria growth was allowed n the case of Pseudomonas aeruginosa in presence of Zn.

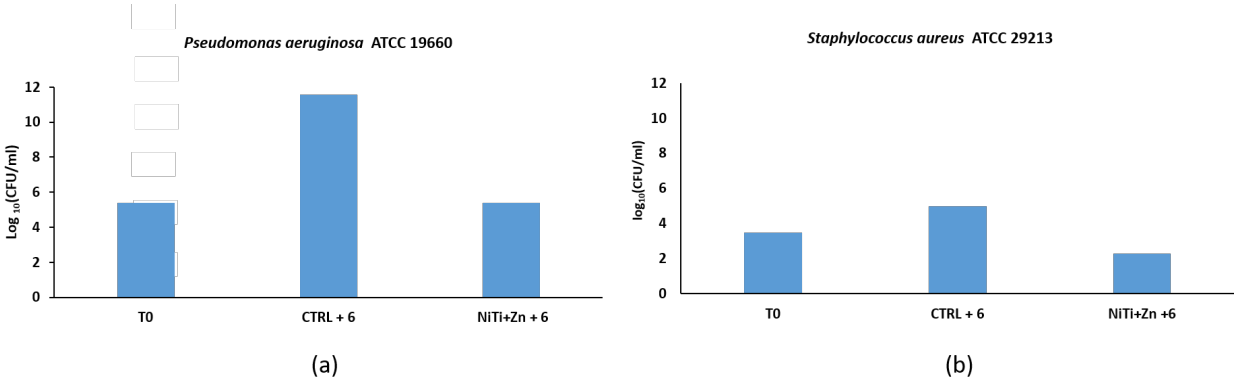

Figure 7: Antibacterial response of the NiTiZn samples, compared with the control (the reference was NiTi) within 6 hours with pseudomonas aeruginosa (a) and Staphylococcus aureus (b).

Conclusions

Laser Powder Bed Fusion process confirmed to be a suitable Additive Manufacturing technology for producing full dense or near full dense NiTi Shape Memory Alloy parts with functional properties. The addition of Zn into NiTi powder allowed to achieve high relative density values, even though its vaporization takes place during the scanning of the powder bed with the laser beam. However, the presence of Zn powder on the border allowed to promote an antibacterial behaviour with higher performances with respect to the undoped NiTi alloy. The operating temperatures were comparable in the samples built with NiTiZn and NiTi powders, while an improvement of the superelasticity was appreciated in the NiTiZn samples then in the NiTi samples. It can be concluded that Zn can be potentially used as antibacterial element to be added to NiTi powder for manufacturing advanced implants. The type of bacterium showed different antibacterial response of the NiTi-Zn alloy; this effect suggests that further investigations are required for better understanding of the biological response of this novel functional alloy for realizing advanced permanent implants.

Acknowledgements

The authors would like to acknowledge Massimo Arosio and Vincenza Ragone for their precious discussions. The authors would like to thank Mayur Nitin Jagdale from Politecnico di Milano, Nicola Bennato and Enrico Bassani from CNR ICMATE for their support in the experimental activity.

References

[1] Funakubo, H.: Shape Memory Alloys, Gordon and Breach Science Publishers, Amsterdam, (1987).
[2] S.A. Shabalovskaya, Biomed. Mater. Eng. 12 (2002) 69-109.
[3] J.X. Xiong,, Y.C. Li, X.J. Wang, P.D. Hodgson, C.E. Wen, J. Mech. Behav. Biomed. Mater. I (2008) 269-273. https://doi.org/10.1016/j.jmbbm.2007.09.003

[4] S. Thomas, Y. Grohens, N. Ninan, in: A.R. Unnithan, R.S. Arathyram, C.S. Kim (Eds.), Scaffolds With Antibacterial Properties, Elsevier Inc., New York (2015), pp. 103-120. https://doi.org/10.1016/B978-0-323-32889-0.00007-8
[5] Erlin Zhang, Xiaotong Zhao, Jiali Hu, Ruoxian Wang, Shan Fu, Gaowu Qin,Antibacterial metals and alloys for potential biomedical implants,Bioactive Materials,Volume 6, Issue 8,2021,2569-2612. https://doi.org/10.1016/j.bioactmat.2021.01.030
[6] M. Saugo, D.O. Flamini, L.I. Brugnoni, S.B. Saidman, Silver deposition on polypyrrole films electrosynthesised onto Nitinol alloy. Corrosion protection and antibacterial activity, Materials Science and Engineering: C, Volume 56, 2015, 95-103, ISSN 0928-4931, https://doi.org/10.1016/j.msec.2015.06.014
[7] Yongkui Yin, Ying Li, Xu Zhao, Wei Cai, Jiehe Sui, One-step fabrication of Ag@Polydopamine film modified NiTi alloy with strong antibacterial property and enhanced anticorrosion performance, Surface and Coatings Technology, Volume 380, 2019, 125013, ISSN 0257-8972. https://doi.org/10.1016/j.surfcoat.2019.125013
[8] Pipattanachat, S., Qin, J., Rokaya, D. et al. Biofilm inhibition and bactericidal activity of NiTi alloy coated with graphene oxide/silver nanoparticles via electrophoretic deposition. Sci Rep 11, 14008 (2021). https://doi.org/10.1038/s41598-021-92340-7
[9] J. Ye, B. Li, M. Li, Y. Zheng, S. Wu, Y. Han, Acta Biomater 107 (2020) 313-324. https://doi.org/10.1016/j.actbio.2020.02.036
[10] K. Yusa, O. Yamamoto, M. Iino, H. Takano, M. Fukuda, Z. Qiao, T. Sugiyama, Arch. Oral Biol. 71 (2016) 162-169. https://doi.org/10.1016/j.archoralbio.2016.07.010
[11] Bassani, P.; Fiocchi, J.; Tuissi, A.; Biffi, C.A. Investigation of the Effect of Laser Fluence on Microstructure and Martensitic Transformation for Realizing Functionally Graded NiTi Shape Memory Alloy via Laser Powder Bed Fusion. Appl. Sci. 2023, 13, 882. https://doi.org/10.3390/app13020882
[12] Farber, E., Zhu, J. N., Popovich, A., & Popovich, V. (2020). A review of NiTi shape memory alloy as a smart material produced by additive manufacturing. Materials Today: Proceedings, 30, 761-767. https://doi.org/10.1016/j.matpr.2020.01.563
[13] Safaei, K., Abedi, H., Nematollahi, M., Kordizadeh, F., Dabbaghi, H., Bayati, P., Reza Javanbakht, Ahmadreza Jahadakbar, Mohammad Elahinia Poorganji, B. (2021). Additive manufacturing of NiTi shape memory alloy for biomedical applications: review of the LPBF process ecosystem. Jom, 73, pages3771-3786 (2021). https://doi.org/10.1007/s11837-021-04937-y
[14] A.G. Demir, P. Colombo, B. Previtali, From pulsed to continuous wave emission in SLM with contemporary fiber laser sources: effect of temporal and spatial pulse overlap in part quality, Int. J. Adv. Manuf. Technol. (2017) 1-14. https://doi.org/10.1007/s00170-016-9948-7
[15] Mahalakshmi S, Hema N, Vijaya P.P., In Vitro Biocompatibility and Antimicrobial activities of Zinc Oxide Nanoparticles (ZnO NPs) Prepared by Chemical and Green Synthetic Route- A Comparative Study. BioNanoScience (2020) 10:112-121 https://doi.org/10.1007/s12668-019-00698-w
[16] ASTM E2180-07 (2012): Test method for evaluation of the activity of antimicrobial agent in polymeric or hydrophobic material.
[17] Biffi, C. A., Fiocchi, J., Sisto, F., Bregoli, C., & Tuissi, A. (2023). Enhanced antibacterial response in Zn-modified additively manufactured NiTi alloy. Materials Letters, 335, 133749. https://doi.org/10.1016/j.matlet.2022.133749